USING CONVOLUTIONAL NEURAL NETWORK (CNN) FOR COVID-19 CHEST X-RAY DIAGNOSIS

Le Thuy Phuong Nhu*, Nguyen Thanh Huy
Ho Chi Minh City University of Education

ARTICLE INFO

Received: 23/9/2023
Revised: 06/11/2023
Published: 06/11/2023

KEYWORDS

Chest X-rays
COVID-19 detection
Image classification
Deep learning
ResNet101

ABSTRACT

Artificial intelligence (AI) was used in chest X-ray (CXR) picture data categorization to brush on accuracy in diagnosing and promptly detecting pneumonia caused by COVID-19. The purpose of this study is to center on developing computer vision which basis for programs for the discovery of radiological features related to COVID-19 on the radiological pictures of the lungs and helps doctors provide appropriate treatment measures to reduce mortality. Over time, CNNs have consistently outperformed other image classification algorithms. Therefore, three architectures based on CNNs including VGG16, ResNet50, and ResNet101 were used to support the successful diagnosis of COVID-19 pneumonia on CXR images. Among them, the best classification performance is the ResNet101 model in terms of average Accuracy and Loss function which are obtained as 95.42% and 0.1492, respectively. Additionally, ResNet101 performed well in classifying the COVID-19 cases in the test dataset with a Precision, Recall, and F1-score of 92.2%, 94.0%, and 93.0%, respectively. Hence, the ResNet101 model can help in clinical practice by building a website that facilitates health professionals to save time and reduce manual errors during the diagnosis.

SỬ DỤNG MẠNG NEURAL TÍCH CHẬP (CNN) ĐỂ CHẨN ĐOÁN COVID-19 TỪ ẢNH X-QUANG NGỰC

Lê Thuý Phương Như*, Nguyễn Thanh Huy
Trường Đại học Sư phạm Thành phố Hồ Chí Minh

THÔNG TIN BÀI BÁO

Ngày nhận bài: 23/9/2023
Ngày hoàn thiện: 06/11/2023
Ngày đăng: 06/11/2023

TỪ KHÓA

X-quang ngực
Phát hiện COVID-19
Phân loại ảnh
Học sâu
ResNet101

TÓM TẮT

Trí tuệ nhân tạo AI được dùng trong phân loại dữ liệu ảnh X-quang ngực nhằm cải thiện độ chính xác trong việc chẩn đoán và phát hiện kịp thời bệnh viêm phổi do COVID-19. Mục đích của nghiên cứu này là phát triển thị giác máy tính dựa trên các chương trình phát hiện các đặc điểm X-quang ngực giúp các bác sĩ đưa ra các biện pháp điều trị phù hợp để giảm tình trạng tử vong. Theo thời gian, mạng neural tích chập hoạt động tốt hơn các thuật toán phân loại hình ảnh khác. Do đó, ba kiến trúc mạng neural gồm VGG16, ResNet50 và ResNet101 được dùng để hỗ trợ chẩn đoán viêm phổi do COVID-19 dựa vào X-quang ngực. Trong số đó, hiệu suất phân loại tốt nhất là ResNet101 với độ chính xác Accuracy và tỷ lệ lỗi Loss thu được lần lượt là 95,42% và 0,1492. Ngoài ra, ResNet101 thể hiện tốt trong việc phân loại các trường hợp COVID-19 trong tập kiểm tra với Precision, Recall và F1-score lần lượt là 92,2%, 94,0% và 93,0%. Chính vì vậy, mô hình ResNet101 có thể hỗ trợ thực hành lâm sàng thông qua việc xây dựng trang web giúp các chuyên gia y tế tiết kiệm thời gian và giảm thiểu các lỗi thủ công trong quá trình chẩn đoán.

DOI: https://doi.org/10.34238/tnu-jst.8810

* Corresponding author. *Email: phuongnhu.lethuy@gmail.com*

1. Introduction

One of the largest global pandemics is COVID-19, which caused tremendous damage to health, economy, and society. Vietnam as well as globally appears to have a good hold on the spread of COVID-19, however, sequelae of post-COVID syndrome have remained, and respiratory infection is the primary clinical manifestation [1].

In reality, the infection caused by COVID-19 could lead to a speedily evolving and potentially deadly pneumonia if COVID-19 pneumonia isn't detected in time or sometimes not given enough attention. Besides, if the reason for pneumonia can't be identified, the treatment behind it will face many challenges because COVID-19 virus infection has a different line from the treatment [2], [3].

Therefore, the early diagnosis and treatment of pandemic coronavirus pneumonia is paramount. Radiologists typically carry out this process [4]. However, the current percentage of doctors is minimal, so it is difficult to meet the needs of society as the number of patients increased remarkably. Moreover, reading the X-ray results depends a lot more on the experience of that doctor than on the experience of many doctors around the world combined. The discrimination of viral, bacterial pneumonia, and especially COVID-19 on radiological imaging is a quite challenging assignment that demands tremendous experience and strong competency in the sector of radiology. Meanwhile, COVID-19 only appeared a few years ago, so the experience of doctors in this field has not been too much and hasn't been done for too long, not to mention the rapidly progressing COVID-19 epidemic. This leads to the doctor making a correct or incorrect diagnosis and the subsequent treatment is affected as well.

To overcome the above problems, scientists have proposed a method of using artificial intelligence (AI) to detect patients affected with COVID-19 pneumonia through CXRs. AI is a speedily increasing sector of computer science with numerous applications for health care. Machine learning is a subset of AI that utilizes deep learning with neural network algorithms. It can not only realize images but also obtain complicated computational assignments often far quicker and with a brush on accuracy than radiologists [5]. When it comes to the effective detection of pneumonia caused by COVID-19, many previous studies [6] - [10] have used several models such as ResNet50 combined with SVM, VGG19 combined with BRISK and RF, ResNet18, ResNet152, VGG16, ResNet101,... The selected deep learning models in this study are VGG16, ResNet50, and ResNet101 because these subjects are considered high accuracy when compared with some other existing deep learning approaches for COVID-19 CXR diagnosis [11], [12].

Hence, this study builds an application to assist doctors in the diagnosis and treatment of pneumonia based on CXR in COVID-19 patients from the COVID-QU-Ex database.

2. Dataset and methods

2.1. COVID-QU-Ex Dataset

In the present study, a collection total of 33,920 CXR pictures have been assessed which were acquired from the public repositories supplied by Qatar University. Some X-ray images including COVID-19 pneumonia, non-COVID infections, and Normal were shown in Figure 1.

These CXR pictures are divided into three groups. Group 1 which contained 11,956 CXR pictures of COVID-19 contagious patients was labeled as COVID-19 pneumonia. Group 2 comprised 11,263 CXR pictures of these patients diagnosed with viral or bacterial pneumonia without COVID-19 contagion that were labeled as non-COVID infections. Group 3 included 10,701 CXR pictures that had no radiological abnormality and it was labeled as Normal [13], [14].

The publicly available X-ray dataset was divided into three parts that consisted of Training set (64.02% of the overall dataset, i.e., 21,715 pictures), Validation Set (15.97% of the overall dataset, i.e., 5,417 pictures), and Testing set (20.01% of the overall dataset, i.e., 6,788 pictures).

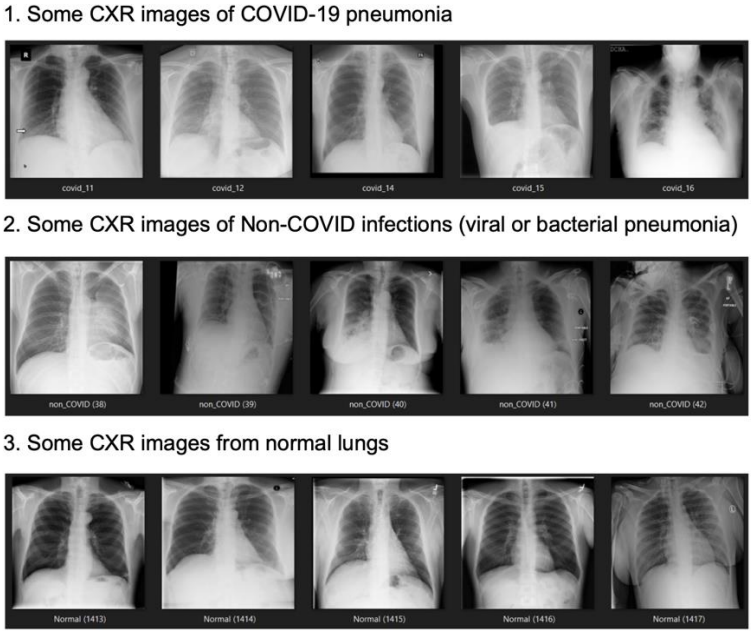

Figure 1. *Images of chest X-rays of patients*

2.2. Methods

2.2.1. Preprocessing

Before applying as input to the models, CXR pictures were resized. Different CNNs have different input requirements. All pictures were standardized followed by the pre-trained neural network norms. Regarding ResNet50, the pictures were resized to 336×336 pixels while for VGG16 and ResNet101, the size of the pictures was 224×224 pixels.

Because all the pictures were in Red–Green–Blue (RGB) format, this study transferred them into another form and displayed grayscale images to facilitate calculation as well as deployment with other datasets. It means that this study modified the shape of the images from (224×224×3) to (224×224×1), as illustrated in Figure 2. The actual size of the image which is (224×224×3) is shown in Figure 2(a) and the modified image which is (224×224×1) is presented in Figure 2(b).

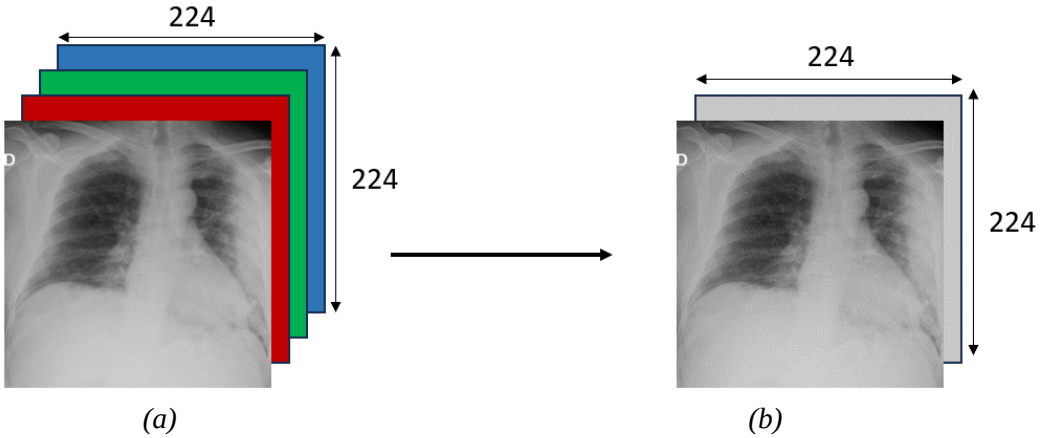

Figure 2. *CXR RGB image (256×256×3) size (a) and CXR gray-scale image with shape (256×256×1) (b)*

2.2.2. Augmentation

Image augmentation is a useful technique that enables the creation of duplicate images with variations. If a deep neural network model only trains on such datasets, the accurate categorization of medical conditions could not yield the desired results which often over-fit the majority class samples' data. Thus, data augmentation is often performed on the training data, allowing the model to learn from more data.

To address the issue and increase the dataset sizes, this study selected a list of the position augmentation techniques including horizontal flip, vertical flip, and random rotate, presented in Table 1.

Table 1. *The distinct parameters for Image augmentations*

Type of Augmentation	Description
horizontal flip	A random horizontal flip is applied with a probability of 0.5.
vertical flip	A random vertical flip is applied with a probability of 0.5.
random rotate	Inputs are randomly rotated with an angle between -0.2 to 0.2 degrees with 75% probability

2.2.3. Classification Models of Lung Images

The flow diagram explains the way how CXR dataset are classified for diagnosis of pneumonia (Figure 3). The parameters that were used during the training phase are mentioned in Table 2.

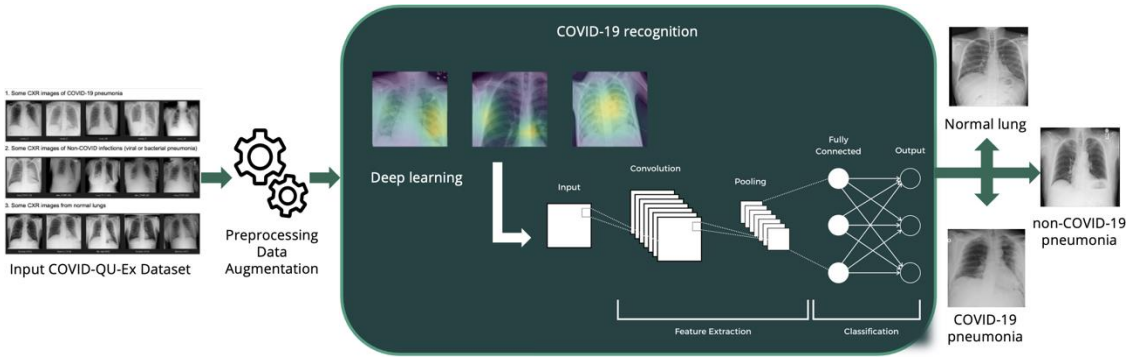

Figure 3. *The flow diagram of the proposed method for discrimination of COVID-19 pneumonia, non-COVID infection, and Normal CXR images.*

Table 2. *The different parameters used during the feature extraction model training process*

Variables	Values
Optimizer	Adam
Learning rate	0.0001
Loss function	Categorical cross-entropy
Evaluation matrix	Accuracy
Image pre-processing	Horizontal flip, Vertical Flip, and Random Rotate
Callbacks	Model checkpoint
Epochs	40
Batch _ size	32

The selected deep learning models are VGG16, ResNet50, and ResNet101. Initially, when it comes to VGG16 CNN architecture, it has a depth of 16 weight layers including 13 convolution layers (conv) and 3 fully connected layers (fc). As can be seen from Figure 4, the VGG16 model

concentrates on having conv of 3×3 filter with a stride 1 and always uses the same padding and max pool layer of 2×2 filter of stride 2. During the overall architecture, the convolution and max pool layers were consistently arranged. The last architecture is 2 fc followed by a softmax for output. The parameters of VGG16 Architecture are quite large with 138 million (approx) parameters [15].

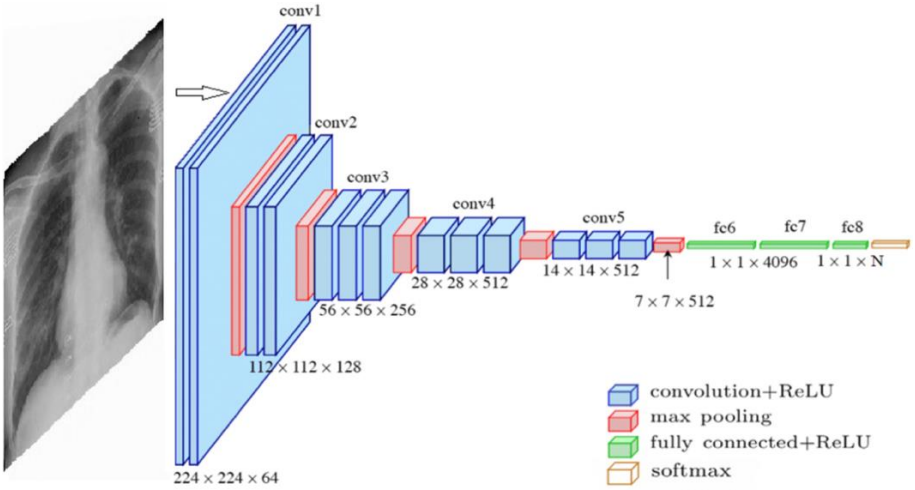

Figure 4. *VGG16 Architecture*

Regarding residual neural network 50 (ResNet50), it has 50 deep layers including 48 conv, 1 max pool, and 1 average pool layer. Figure 5 depicts the arrangement of sequences of conv, max pool, average pooling, and fully connected layer of the ResNet50 model in which average pooling is used to decrease the size of the picture input to the network, followed by a softmax activation as at the final layer for categorization. Most strikingly, the residual layers and skip connections feature of this network can help brush on accuracy and can overcome the problem of gradient loss which may result in stopping the weight on the model for further updates or changes [11], [16].

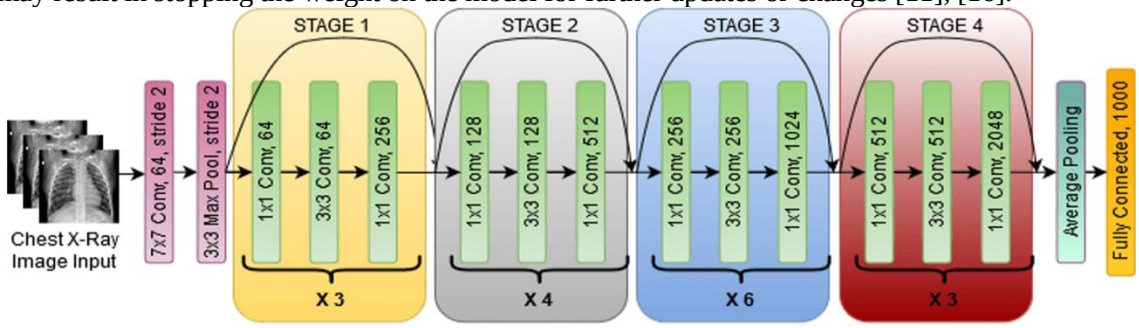

Figure 5. *ResNet50 Architecture*

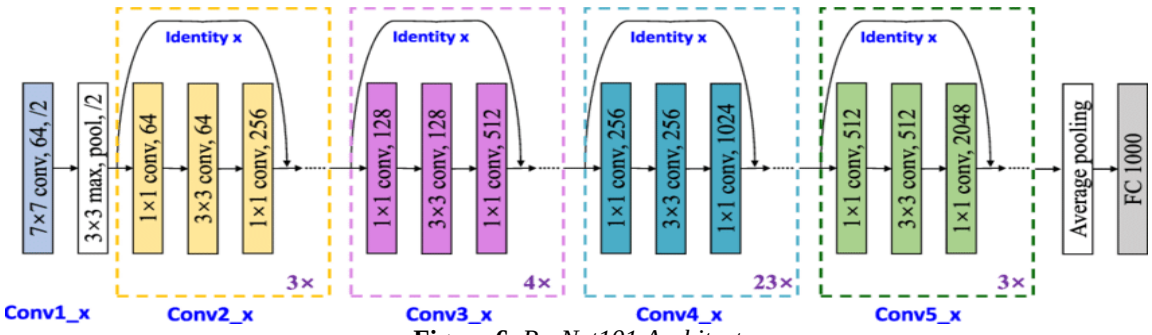

Figure 6. *ResNet101 Architecture*

Ultimately, ResNet101 architecture has 101 deep layers comprised of five convolution layers (namely conv1_x, conv2_x, conv3_x, conv4_x, and conv5_x) and 1 fc (Figure 6). This arrangement brings its learning framework advantage that is known to have lower computational complexity than its counterpart, without getting rid of the depth and in turn the accuracy [17].

2.2.4. Evaluation Metrics

As far as estimating the performance of the proposed models in this research is concerned, a confusion matrix that includes Accuracy, Precision, Recall, and F1-score was utilized [11], [16]. The following equation measures the performance metrics,

$$\text{Accuracy} = \frac{\text{TP+ TN}}{\text{TP + TN + FP + FN}} \quad (1)$$

$$\text{Precision} = \frac{\text{TP}}{\text{TP + FP}} \quad (2)$$

$$\text{Recall} = \frac{\text{TP}}{\text{TP + FN}} \quad (3)$$

$$\text{F1-score} = \frac{2 \times \text{Precision x Recall}}{\text{Precision + Recall}} \quad (4)$$

where TP presents COVID-19 picture data categorized correctly, FP presents normal picture data incorrectly categorized as COVID-19 by the proposed system, TN presents normal picture data categorized as COVID-19 correctly, and FN presents the COVID-19 picture data is incorrectly categorized as a normal case.

To categorize the real pictures from the fake pictures, this study used binary cross-entropy as the loss function, indicated by Equation (5) in which M is the number of training CXR pictures in a mini-batch, ym is the target label for training picture m (the real label is 1 and the fake label is 0), xm is the input for training picture m, and $h\theta$ is the model with neural network weights θ [18].

$$J(\theta) = -\frac{1}{M}\sum_{m=1}^{M}\left[ym \times \log\left(\text{h}\theta\ (xm)\right) + (1 - ym) \times \log\left(1 - \text{h}\theta\ (xm)\right)\right] \quad (5)$$

2.2.5. GUI Application Design

Based on the performance of the models and the data, a website was created to assess CXR for COVID-19 by using Streamlit which is an open-source app framework in Python language.

3. Results and Discussion

3.1. Training of deep classification networks

For the purpose of assessing the computational complexity of the deep function extraction models, this study compares the training time of those models, as indicated in Table 3.

Table 3. *Differences between the training time of considered CNN models*

Model	Training time (hour)	Inference time (second)
VGG16	3.78	0.32s
ResNet50	6.67	0.56s
ResNet101	8.2	0.85s

The VGG16 model took 3.78 hours for training, with an average inference per image is 0.32s. The ResNet50 training was completed in 6.67 h with 0.56s as the inference time by second. The ResNet101 network needs the highest training time of 8.2 h with 0.85s for the inference stage.

3.2. Experimental results

Among the deep neural network trained on 21,715 CXR images, VGG16 and ResNet50 are equally performing for classifying images while ResNet101 is performing better than others, as illustrated in Table 4. As seen from Table 4, the detection of the ResNet101 model in the COVID-19 class is higher than the other models via the Accuracy and Loss values obtained as 95.42% and 0.1492, respectively.

Table 4. *Experimental results obtained with different deep-learning methods*

Model	Accuracy (%)	Loss
VGG16	94.22	0.1714
ResNet50	94.39	0.1561
ResNet101	**95.42**	0.1492

Figure 7, Figure 8, and Figure 9 below give information about the comparative line graphs of models results on Training data and Validation data of metrics in terms of the Accuracy and Loss of ResNet101, ResNet50, and VGG16, respectively.

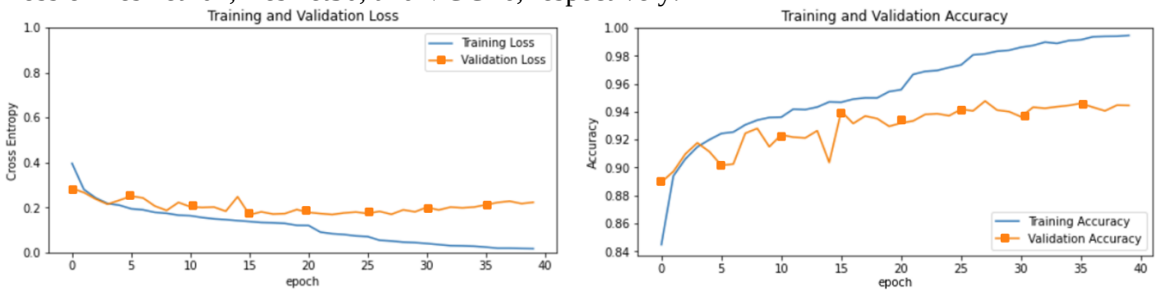

(a) *(b)*

Figure 7. *Graphical comparison of Training and Validation Loss (a) and graphical representation of Training and Validation Accuracy (b) of the ResNet101*

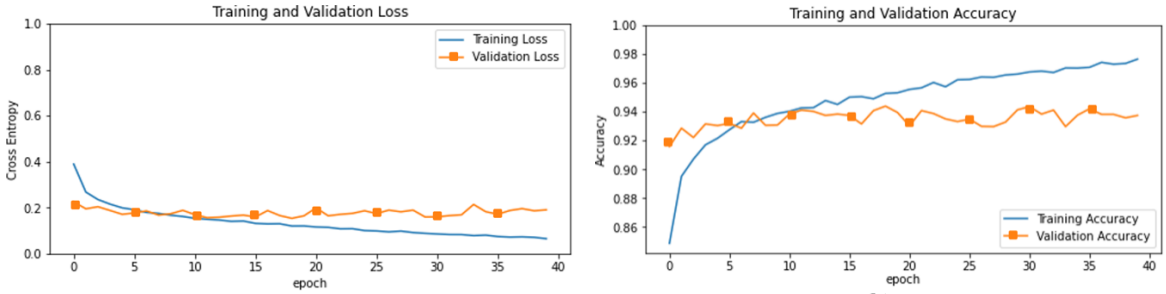

(a) *(b)*

Figure 8. *Graphical comparison of Training and Validation Loss (a) and graphical representation of Training and Validation Accuracy (b) of the ResNet50*

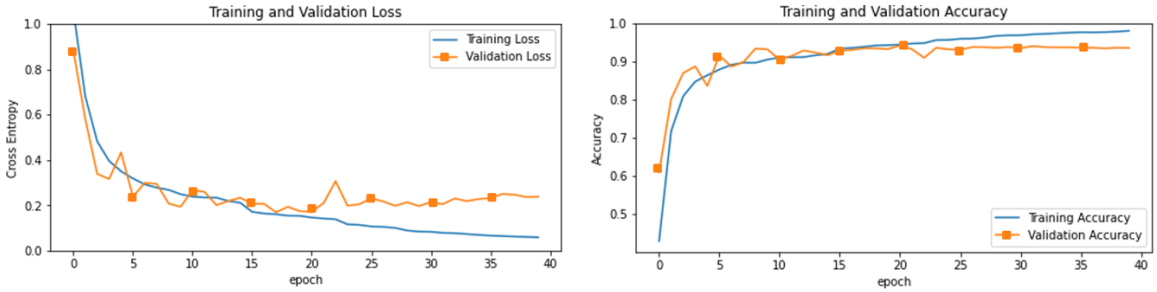

(a) *(b)*

Figure 9. *Graphical comparison of Training and Validation Loss (a) and graphical representation of Training and Validation Accuracy (b) of the VGG16*

Firstly, as seen in Figure 7, the ResNet101 model appears to achieve the highest result after the 12th epoch with an Accuracy of 95.42% and a Loss of 0.1492. Secondly, from Figure 8 it is clear that the 18th epoch witnesses the highest performance of the ResNet50 model provided Accuracy and Loss of 94.39%, and 0.1561, respectively. The Accuracy of the ResNet50 model fluctuated, although it always remained above 93% toward the end of the epoch number. Finally, Figure 9 presents that the VGG16 model reached an Accuracy of 94.22% and a Loss of 0.1714 in

the 21st epoch. In Figure 10, it can be seen that among the three architectures, ResNet101 achieved the best performance with 95.42 %, 92.2%, 94.0%, and 93.0% on Accuracy, Precision, Recall, and F1-score, respectively. Due to the balanced dataset, our model shows its stability with a small variance among these metrics. According to 91.2%, 91.8%, and 93.0% on the F1-score metric, the dataset might require deeper architecture like ResNet101 for well-represented feature extraction. Based on the visualization of the confusion metric of ResNet101, the model has promising results when the performance on the COVID-19 class is the most correct on the test set, with 1848 correct cases over 1,903 predictions. Even though the model finds it hard to differentiate between non-COVID and Normal, it still shows robustness by conducting good classification with 1,650 and 1,556 true positive predictions.

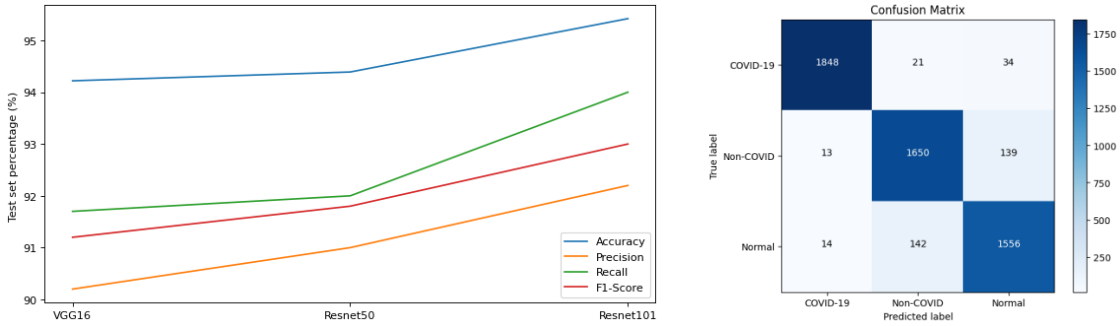

(a) *(b)*

Figure 10. *Experimental results comparison between three architectures with 4 evaluation metrics (a) and confusion metric of the ResNet101 with three classes prediction (b)*

3.3. Comparison with other studies

In order to detect COVID-19 pneumonia, non-COVID infections, and Normal lung from CXR pictures, many previous studies have used several models such as ResNet50 combined with SVM, VGG19 combined with BRISK and RF, ResNet18, ResNet152, VGG16, ResNet101,... With the ResNet101 model, the subject attained a maximum accuracy of 95.42%, which is considered high when compared with some other existing state-of-the-art deep learning methods for detecting COVID-19 with CXR pictures, presented in Table 5.

Table 5. *Comparison with the other existing state-of-art approaches in terms of accuracy rate for classification of CXR images*

Authors	Method	Dataset	Accuracy (%)
Sethy & Behera, 2020 [6]	ResNet50 + SVM	127 images for 3 classes: COVID, Pneumonia, Normal	95.38
Bhattacharyya, 2022 [7]	VGG19, BRISK + RF	342 COVID, 341 Normal and 347 Pneumonia images	96.6
Yoo, 2020 [8]	ResNet18	COVID-Chest Xray-Dataset	95.0
Albahli, 2020 [9]	ResNet152	84,312 images with 8 diseases classes	87.0
Civit-Masot, 2020 [10]	VGG16	5,887 images of 3 classes healthy, pneumonia and COVID-19	86.0
Proposed method	ResNet101	COVID-Qu-Ex dataset with 33,920 images of 3 classes	95.42

3.4. GUI Design for application

In comparison to other models, the result of the ResNet101 model is better because it has an Accuracy of about 95.42% and a very low Loss of about 0.1492. As a result, the ResNet101 model was used to create a website that runs on mobile as well as desktop platforms to augment

COVID-19 CXR diagnosis. Figure 11 below shows the web interface and use of this website. In the first step, a user can drag and drop the CXR image file which has both an upload limit of less than 200MB in size and a JPG (or PNG) format. After that, the machine learning algorithm would provide the probability of COVID-19 pneumonia, non-COVID infections, or Normal lung diagnosis. Finally, it is based on this probability for making a final diagnosis of the patient.

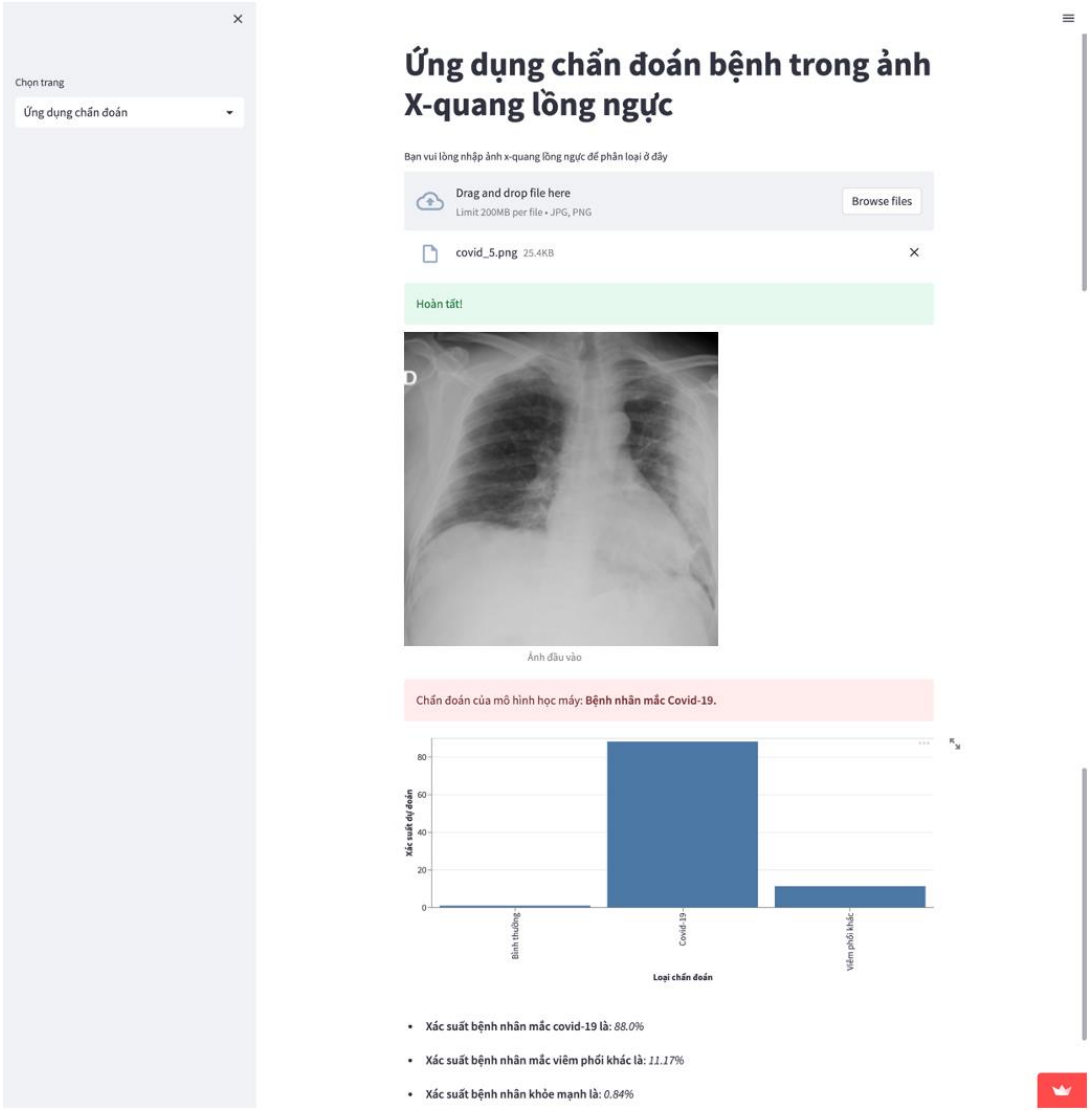

Figure 11. *Artificial Intelligence Research Website*

4. Conclusion

In summary, the early diagnosis of COVID-19 pneumonia plays an imperative for early interference with the patient. For this study, 33,920 CXR images obtained from COVID-19 pneumonia, non-COVID-19 infections, and Normal are classified using the three models including ResNet101, ResNet50, and VGG16. Among them, the highest classification Accuracy rate is the ResNet101 model, with 95.42%, compared to 94.39% and 94.22% for the ResNet50 and VGG16 models. Moreover, ResNet101 exhibits exceptionally well in classifying the COVID-19 cases in the test dataset with a Precision of 92.2%, Recall of 94.0%, and F1-score of 93.0%. Consequently, ResNet101 was used to create a website that could assist radiologists as a second diagnostic tool to enhance the classification accuracy rate.

REFERENCES

[1] A. Pavli, M. Theodoridou, and H. C. Maltezou, "Post-COVID Syndrome: Incidence, Clinical Spectrum, and Challenges for Primary Healthcare Professionals," *Archives of Medical Research*, vol. 52, no. 6, pp. 575–581, Aug. 2021.

[2] A. M. Tahir, M. E. Chowdhury, A. Khandakar, T. Rahman, Y. Qiblawey, U. Khurshid, S. Kiranyaz, N. Ibtehaz, M. S. Rahman, S. Al-Maadeed, S. Mahmud, M. Ezeddin, K. Hameed, and T. Hamid, "COVID-19 infection localization and severity grading from chest X-ray images," *Computers in Biology and Medicine*, vol. 139, Dec. 2021, Art. no. 105002.

[3] G. Jain, D. Mittal, D. Thakur, and M. K. Mittal, "A deep learning approach to detect Covid-19 coronavirus with X-Ray images," *Biocybernetics and Biomedical Engineering*, vol. 40, no. 4, pp. 1391–1405, Oct. 2020.

[4] J. Pedrosa, G. Aresta, C. Ferreira, C. Carvalho, J. Silva, P. Sousa, L. Ribeiro, A. M. Mendonça, and A. Campilho, "Assessing clinical applicability of COVID-19 detection in chest radiography with deep learning," *Sci. Rep.*, vol. 12, no. 1, Apr. 2022, Art. no. 6596.

[5] A. A. Borkowski, N. A. Viswanadhan, L. B. Thomas, R. D. Guzman, L. A. Deland, and S. M. Mastorides, "Using Artificial Intelligence for COVID-19 Chest X-ray Diagnosis," *Federal Practitioner*, vol. 37, no. 9, pp. 398–404, Sep. 2020.

[6] P. K. Sethy and S. K. Behera, "Detection of Coronavirus Disease (COVID-19) Based on Deep Features," Preprints, Mar. 19, 2020.

[7] A. Bhattacharyya, D. Bhaik, S. Kumar, P. Thakur, R. Sharma, and R. B. Pachori, "A deep learning based approach for automatic detection of COVID-19 cases using chest X-ray images," *Biomedical Signal Processing and Control*, vol. 71, Jan. 2022, Art. no. 103182.

[8] S. H. Yoo, H. Geng, T. L. Chiu, S. K. Yu, D. C. Cho, and J. Heo, "Deep Learning-Based Decision-Tree Classifier for COVID-19 Diagnosis From Chest X-ray Imaging," *Front Med (Lausanne)*, vol. 7, Jul. 2020, Art. no. 427.

[9] S. Albahli, "A Deep Neural Network to Distinguish COVID-19 from other Chest Diseases using X-ray Images," *Current Medical Imaging*, vol. 17, no. 1, pp. 109-119, Jun. 2020.

[10] J. Civit-Masot, F. Luna-Perejón, M. D. Morales, and A. Civit, "Deep Learning System for COVID-19 Diagnosis Aid Using X-ray Pulmonary Images," *Applied Sciences*, vol. 10, no. 13, Jan. 2020, Art. no. 4640.

[11] D. Reynaldi, B. S. Negara, S. Sanjaya, and E. Satria, "COVID-19 Classification for Chest X-Ray Images using Deep Learning and Resnet-101," in *2021 International Congress of Advanced Technology and Engineering (ICOTEN)*, Jul. 2021, pp. 1–4.

[12] A. V. Ikechukwu, S. Murali, R. Deepu, and R. C. Shivamurthy, "ResNet-50 vs VGG-19 vs training from scratch: A comparative analysis of the segmentation and classification of Pneumonia from chest X-ray images," *Global Transitions Proceedings*, vol. 2, no. 2, pp. 375–381, Nov. 2021.

[13] M. E. H. Chowdhury, T. Rahman, A. Khandakar, R. Mazhar, M. A. Kadir, Z. B. Mahbub, K. R. Islam, M. S. Khan, A. Iqbal, N. A. Emadi, M. B. I. Reaz, and M. T. Islam, "Can AI Help in Screening Viral and COVID-19 Pneumonia?," *IEEE Access*, vol. 8, pp. 132665–132676, 2020.

[14] T. Rahman, A. Khandakar, Y. Qiblawey, A. Tahir, S. Kiranyaz, S. B. A. Kashem, M. T. Islam, S. A. Maadeed, S. M. Zughaier, M. S. Khan, and M. E. H. Chowdhury, "Exploring the effect of image enhancement techniques on COVID-19 detection using chest X-ray images," *Computers in Biology and Medicine*, vol. 132, May 2021, Art. no. 104319.

[15] S. Rudregowda, S. P. Kulkarni, G. H. Lokesh, V. Ravi, and M. Krichen, "Visual Speech Recognition for Kannada Language Using VGG16 Convolutional Neural Network," *Acoustics*, vol. 5, no. 1, pp. 343-353, Mar. 2023.

[16] S. Sakib, M. A. B. Siddique, M. M. Rahman Khan, N. Yasmin, A. Aziz, M. Chowdhury, and I. K. Tasawar, "Detection of COVID-19 Disease from Chest X-Ray Images: A Deep Transfer Learning Framework," *Preprints*, Nov. 12, 2020, doi: 10.1101/2020.11.08.20227819.

[17] M. Z. Che Azemin, R. Hassan, M. I. Mohd Tamrin, and M. A. M. Ali, "COVID-19 Deep Learning Prediction Model Using Publicly Available Radiologist-Adjudicated Chest X-Ray Images as Training Data: Preliminary Findings," *International Journal of Biomedical Imaging*, vol. 2020, Aug. 2020, Art. no. e8828855.

[18] S. K. Venu and S. Ravula, "Evaluation of Deep Convolutional Generative Adversarial Networks for Data Augmentation of Chest X-ray Images," *Future Internet*, vol. 13, no. 1, Jan. 2021, Art. no. 8.